The interaction between AMPKβ2 and the PP1-targeting subunit R6 is dynamically regulated by intracellular glycogen content

Yvonne Oligschlaeger[*], Marie Miglianico[*], Vivian Dahlmans[$], Carla Rubio-Villena[#], Dipanjan Chanda[*], Maria Adelaida Garcia-Gimeno[#], Will A. Coumans[*], Yilin Liu[*], J. Willem Voncken[$], Joost J.F.P. Luiken[*], Jan F.C. Glatz[*], Pascual Sanz[#], Dietbert Neumann[*1]

[*]CARIM School for Cardiovascular Diseases, [$]GROW School for Oncology & Developmental Biology, Department of Molecular Genetics, Maastricht, the Netherlands
[#]Instituto de Biomedicina de Valencia, Consejo Superior de Investigaciones Cientificas (CSIC) and Centro de Investigación en Red de Enfermedades Raras (CIBERER), Valencia, Spain

[1]Correspondence:
D. Neumann, Department of Molecular Genetics, CARIM School of Cardiovascular Diseases, Maastricht University, 6200 MD Maastricht, The Netherlands; Tel. +3143388-1851; Fax. +3143388-4574; E-mail: d.neumann@maastrichtuniversity.nl

ABSTRACT
AMP-activated protein kinase (AMPK) is a metabolic stress-sensing kinase. We previously showed that glucose deprivation induces autophosphorylation of AMPKβ at threonine-148 (Thr-148), which prevents the binding of AMPK to glycogen. Furthermore, in MIN6 cells, AMPKβ1 binds to R6 (PPP1R3D), a glycogen-targeting subunit of protein phosphatase 1 (PP1), thereby regulating the glucose-induced inactivation of AMPK. Here, we further investigated the interaction of R6 with AMPKβ and the possible dependency on Thr-148 phosphorylation status. Yeast two-hybrid analyses and co-immunoprecipitation of the overexpressed proteins in HEK293T cells revealed that both AMPKβ1 and β2 wild-type (WT) isoforms bind to R6. The AMPKβ/R6 interaction was stronger with the muscle-specific β2-WT and required association with the substrate-binding motif of R6. When HEK293T cells or C2C12 myotubes were cultured in high-glucose medium, AMPKβ2-WT and R6 weakly interacted. In contrast, glycogen depletion significantly enhanced this protein interaction. Mutation of AMPKβ2 Thr-148 prevented the interaction with R6 irrespective of the intracellular glycogen content. Treatment with the AMPK activator oligomycin enhanced AMPKβ2/R6 interaction in conjunction with increased Thr-148 phosphorylation in cells grown in low glucose medium. These data are in accordance with R6 binding directly to AMPKβ2 when both proteins detach from the diminishing glycogen particle, which is simultaneous to increased AMPKβ2 Thr-148 autophosphorylation. Such model points to a possible control of AMPK by PP1-R6 upon glycogen depletion in muscle.

SUMMARY STATEMENT
Breakdown of intracellular glycogen enhances interaction of the AMPKβ2 subunit and the R6 glycogen-targeting subunit of the protein phosphatase-1 (PP1), which occurs in conjunction with increased β2-threonine-148 phosphorylation.

SHORT TITLE
Glycogen-dependent regulation of AMPKβ2/R6 interaction

KEYWORDS
AMP-activated protein kinase (AMPK), R6, glycogen targeting, protein-protein interaction, phosphorylation, glycogen metabolism

ABBREVIATIONS

ACC, Acetyl-CoA Carboxylase; AICAR, 5-Aminoimidazole-4-carboxamide ribonucleotide; AMPK, AMP-activated protein kinase; ATP, adenosine triphosphate; β-CD, β-cyclodextrin; CBM, Carbohydrate-binding module; EV, empty vector; GP, Glycogen phosphorylase; GS, Glycogen synthase; HEK293T, human embryonic kidney 293T cell line; iFCS, heat-inactivated calf serum; IP, Immunoprecipitation; PP1, Protein phosphatase type1; R6, PP1-glycogen-targeting subunit PPP1R3D; Snf1, sucrose-non-fermenting 1; Reg1, yeast targeting subunit of PP1; WT, wild-type; Y2H, Yeast two-hybrid.

INTRODUCTION

Muscular tissue, in particular skeletal muscle, is an important site for glucose storage. It has become evident that glucose disposal into glycogen is essential for coordinated glucose homeostasis, as conditions limiting glycogen synthesis are associated with, for instance, hyperglycemia and insulin resistance (1). AMP-activated protein kinase (AMPK) is a metabolic energy sensor that mediates insulin-independent GLUT4 translocation to the plasma membrane resulting in increased glucose uptake (2). Therefore, AMPK activation could normalize blood glucose levels in type 2 diabetic patients. In response to various cellular stresses (*e.g.*, contraction, nutrient-deprivation), AMPK is activated and modulates downstream targets to induce catabolic, ATP-producing processes and inhibit anabolic, ATP-consuming processes, thereby restoring energy homeostasis. AMPK consists of three subunits, the catalytic α subunit, and two regulatory β and γ subunits; the latter are essential for regulating AMPK activity, as well as subcellular localization. AMPK subunits occur in different isoforms (α1, α2; β1, β2; γ1, γ2, γ3) partly showing a tissue-specific expression pattern. Namely, β2 is the predominant isoform found in heart and skeletal muscle (3, 4). Accordingly, it has been reported that β1 knockout mice have a minimal phenotype in skeletal muscle (5), whereas β2 knockout mice have reduced skeletal muscle AMPK activity, exercise capacity and glucose uptake (6, 7).

AMPK is known to shuttle between the nucleus (8, 9) and the cytoplasm (10, 11), suggesting that AMPK exerts compartment-specific effects in order to monitor and coordinate complex cell biological processes. The β subunit carbohydrate-binding module (CBM) allows AMPK to associate with glycogen (12, 13), where it interacts with other glycogen-binding proteins including glycogen synthase (GS) (13) and glycogen phosphorylase (GP) (12). Notably, β2 shows higher affinity for glycogen compared to β1 (14). Acute 5-Aminoimidazole-4-carboxamide ribonucleotide (AICAR)-induced AMPK activation inactivates GS via Ser7 phosphorylation in skeletal muscle (15), although high levels of glucose-6-phosphate can override this inhibition (16).

The regulation of the activity status of localized AMPK is dependent on allosteric activation/repression and the action of upstream kinases capable of phosphorylating threonine-172 (Thr-172) in the catalytic α subunit (*e.g.*, LKB1, TAK1, CaMKK2). Several protein phosphatases (*e.g.*, PP1, PP2A, PP2C) dephosphorylate Thr-172, thus leading to AMPK inactivation. PP1 is an important protein phosphatase in mammalian cells that is involved in proper coordination of glycogen metabolism by dephosphorylating target enzymes such as GS and GP. Recruitment of PP1 to its target substrates and to glycogen occurs by means of its glycogen-targeting proteins, such as PTG/R5 (PPP1R3C) (17) or R6 (PPP1R3D) (18, 19). Insight into PP1-mediated AMPK regulation came from our previous study (20), which showed that R6 physically interacts with the AMPKβ1 subunit, resulting in glucose-induced AMPK dephosphorylation by the PP1-R6 complex. Furthermore, we found that the CBM domain within the AMPKβ1 subunit is required for interaction with R6, as substitution of glycine-147 for arginine (G147R) resulted in total loss of AMPK/R6 interaction (20). These results were consistent with parallel studies in yeast showing that Snf1 is regulated by glucose, and that Gal83 via its CBM interacts with Reg1, the orthologs of AMPKβ and R6, respectively (21), thus pointing to an evolutionary conserved mechanism.

We recently reported that autophosphorylation of Thr-148 in the AMPKβ subunit interferes with the recruitment of AMPK to glycogen, suggesting that AMPK-glycogen localization is tightly regulated and linked to glycogen storage (22). Given the direct binding of AMPKβ1 to R6 and the observed loss of this interaction using the AMPKβ1-G147R mutant, we hypothesized a role for AMPKβ Thr-148

phosphorylation. In this current study, we provide insight into the binding of AMPKβ2 to R6 in relation to glycogen content and AMPKβ2 Thr-148 phosphorylation. Our results indicate that the AMPKβ2/R6 interaction is dynamically controlled by glycogen content.

MATERIALS AND METHODS

Plasmids

For expression in mammalian cells, the cDNA of full-length AMPKβ1 and AMPKβ2 was amplified by PCR and ligated in frame into the pmCherry expression vector (Clontech) via EcoRI and SalI restriction sites, as previously described (22). An AMPKβ2–mCherry construct bearing a threonine-to-aspartate mutation on residue 148 (T148D) was generated using the Quick-change site-directed mutagenesis kit (Stratagene). The pcDNA3 constructs for expression of AMPKγ1 and myc-AMPKα1 were kindly provided by Dr. D. Carling (Imperial College London, London, United Kingdom). The corresponding ORF of AMPKβ2-T148D mutant was subcloned into pBTM116 to allow for expression in yeast (LexA-AMPKβ2-T148D). The pFLAG-R6 construct for mammalian expression of R6-WT and R6-mutants (R6-RARA, -RAHA, -WDNAD and -WANNA) were generated as previously described, and the pFLAG was used as empty vector (EV) control (20, 23).

Other plasmids used for yeast two-hybrid analyses were pGADT7-Φ (GAD, empty plasmid), pGADT7-R6 (GAD-R6), pBTM-R6 (LexA-R6), pBTM-R6-RARA (LexA-R6-RARA), pBTM-R6-RAHA (LexA-R6-RAHA), pBTM-R6-WANNA (LexA-R6-WANNA), pBTM-R6-WDNAD (LexA-R6-WDNAD), pGADT7-AMPKβ1 (GAD-AMPKβ1), pGADT7-AMPKβ2 (GAD-AMPKβ2), pBTM-AMPKβ1 (LexA-AMPKβ1), pBTM-AMPKβ2 (LexA-AMPKβ2) (20, 23-25).

For retroviral overexpression and optimal detection of exogenous β2, full-length AMPKβ2-WT or AMPKβ2-T148D was amplified using PCR primers containing an optimized tetra-cysteine sequence (FlAsH-tag; FLNCCPGCCMEP). First, the corresponding ORF (FlAsH-tag) was subcloned into the SalI and NotI site of the mammalian β2-WT-mCherry or β2-T148D-mCherry construct, exchanging the mCherry-tag for FlAsH-tag. Second, β2-WT-FlAsH or β2-T148D-FlAsH was amplified and subcloned into the EcorI and SalI site of the retroviral pBabe-puromycin retroviral backbone (kindly provided by Dr. G. Nolan, Stanford University, CA).

For retroviral overexpression of R6, the corresponding ORF (R6-WT) was amplified by PCR and subcloned into the BstxI and SalI restriction sites of the pBabe-puromycin retroviral backbone (kindly provided by Dr. G. Nolan, Stanford University, CA). The pBabe-puromycin empty vector (EV) was used as control. Primer sequences are available from the author upon request. All of the constructs were verified by DNA sequencing.

Cell culture

The human embryonic kidney 293T cell line (HEK293T) was cultured in DMEM with high glucose (25 mM) (Gibco), supplemented with 10 % (v/v) heat-inactivated fetal calf serum (iFCS, Bodinco BV, Alkmaar, The Netherlands) and 1 % penicillin/streptomycin (Invitrogen), unless otherwise stated. For transient transfections, HEK293T cells were seeded to 30 % confluence in 6-well plates (Greiner Bio-one) 24 h before transfection. For determination of protein-protein interaction, cells were co-transfected with AMPK (α1-myc, γ1, and β1-WT-mCherry or β2-WT/β2-T148D-mCherry), and/or FLAG-R6 (R6-WT/R6-RARA/R6-RAHA/R6-WANNA/R6-WDNAD) or FLAG empty vector (EV) plasmid DNA using Lipofectamine 2000 (Invitrogen) in antibiotic-free culture medium. Six to eight hours after transfection, transfection medium was replaced by normal growth medium. At 48-72 h after transfection and continuous culturing (*i.e.*, without change of medium), cells were harvested for glycogen or subjected to immunoprecipitation and Western blotting.

In order to induce glycogen depletion, HEK293T cells growing in high glucose medium (DMEM 25 mM glucose, 10 % iFCS), were subjected to forskolin treatment (100 μM, Sigma), low glucose medium (DMEM 3 mM glucose, 10 % iFCS), or glucose-deprived medium (DMEM 0 mM, 10 % iFCS) for 16 h. To activate AMPK, cells were serum-starved in high- (DMEM 25 mM) or low-glucose (3 mM) medium for 16 h, and subsequently treated with oligomycin (3 μM, Sigma) for 1 h.

The mouse skeletal muscle cell line C2C12 was kindly provided by Dr. R.C. Langen (Maastricht University, The Netherlands). C2C12 cells were continuously cultured to approximately 80 % confluence in DMEM with high glucose (25 mM) (Gibco), supplemented with 10 % (v/v) iFCS (Bodinco BV, Alkmaar, The Netherlands) and 1 % penicillin/streptomycin (Invitrogen). For differentiation into myotubes, myocytes (75 - 85 % confluence) were further grown in differentiation medium (DMEM 25 mM glucose (Gibco), supplemented with 2 % heat-inactivated horse serum (Invitrogen, Life Technologies) and 1 % penicillin/streptomycin (Invitrogen) for 4 – 5 days. Subsequently, cells were used in the corresponding experiments. In order to induce glycogen depletion, myotubes were maintained in low glucose medium (DMEM 3 mM glucose, supplemented with 2 % iFCS), for 16 h. In order to activate AMPK, myotubes were maintained in high or low glucose for 16 hours as described above, and subsequently treated with oligomycin (5 μM, Sigma) for 30 min.

Retroviral infections

In order to study protein-protein interactions in C2C12 myotubes, growing cells were infected with FlAsH-tagged AMPKβ2-WT or -T148D, or FLAG-tagged R6 retrovirus. Briefly, retroviral systems and Phoenix helper-free retrovirus producer cell lines were used as published before (26-28). Amphotropic retroviral supernatants were produced as previously described (22). Briefly, 24 - 48 h after calcium phosphate/DNA transfection of producer cells, supernatants were harvested, filtered (0.45 micron filters; Corning, Germany) and used for infection of C2C12 cells in presence of 4 μg/ml polybrene (Sigma). For infections, cells were incubated with virus particles for 6 - 8 h and then allowed to recover for 48 h on fresh medium, before selection pressure was applied. Stably infected cells were selected 2 days post-infection with 4 μg/ml puromycin for 36 – 48 h preceding experiments.

Immunoprecipitation and Western blotting

Immunoprecipitation procedures were performed as previously described (22). Briefly, exogenous myc-AMPKα1 was immunoprecipitated using anti-myc-tag antibody (9B11, Cell Signaling Technology, Beverly, MA), exogenous R6 was immunoprecipitated using anti-FLAG-tag antibody (F3165, Sigma), and endogenous AMPK was immunoprecipitated using a combination of AMPKα1 and AMPKα2 antibodies raised in sheep (kindly provided by Prof. dr. G. Hardie), followed by incubation with protein G-Sepharose beads (GE Healthcare). Western blot analysis was carried out using the following primary antibodies: myc-tag, tAMPKα, AMPKβ1, AMPKβ2, phospho-AMPK-T172 (all from Cell Signaling Technology, Beverly, MA), FLAG-tag (F3165, Sigma), R6 (AP13440a, Abgent), and phospho-AMPKβ2-T148 (22). R6 was detected using FLAG-tag (F3165, Sigma), unless otherwise stated. Detection was performed according to its primary antibody using anti-rabbit (Cell Signaling Technology) and anti-mouse (Dako) horse-radish peroxidase (HRP)-conjugated secondary antibodies, followed by chemiluminescence.

In order to investigate the role of glycogen, myc-AMPKα1 was immunoprecipitated using the anti-myc-tag antibody after the addition of the glycogen-mimic β-cyclodextrin (5 mM, Sigma) for 1 h at 4 °C. Subsequently, immune complexes were electrophoresed by SDS-PAGE and analyzed by Western blot analysis, as described above.

Biochemical intracellular glycogen measurement

Intracellular glycogen content was measured, as previously described (22). Briefly, HEK293T cells (non-transfected or transfected) or stably-infected C2C12 myotubes were lysed in potassium hydroxide (30 %) and boiled at 70 °C for 30 min. Subsequently, samples were cooled to 25 °C before sodium sulfate (6 %, w/v) and EtOH (99.5 %, v/v) were added at a 1:1:3 ratio. After thorough mixing, samples were rotated top-over-top at 4 °C for 30 – 60 min. The precipitate was collected by centrifugation at 5000 rpm (Eppendorf Centrifuge 5415 R) for 5 min at 4 °C. To hydrolyze glycogen, pellets were dissolved in 1 M HCl and boiled at 100 °C for 2 h. Samples were cooled before neutralization using 2 M NaOH. Hydrolysates were used for glucose determination using a glucose (GO) assay kit (Sigma), according to the manufacturer's instructions.

Determination of glucose uptake
The glucose uptake protocol was adapted from earlier work (29). Briefly, stably infected C2C12 myotubes were incubated with the uptake buffer containing deoxy-D-glucose (4 μM), with tracer amounts of ^{3}H-labelled 2-deoxy-D-glucose, for 10 min. Surplus substrate was removed by washing the cells with ice-cold uptake buffer and cells were lysed in 0.1 N sodium hydroxide. Incorporated glucose was assessed by scintillation counting of ^{3}H in lysates.

Preparation of skeletal muscle tissue homogenates
Gastrocnemius muscle was taken from one female wild type C57/BL6 mouse of the regular Maastricht University breeding program. After sacrifice by carbon dioxide inhalation and cervical dislocation, tissues were freeze clamped between aluminum tongs precooled in liquid nitrogen and stored at -80°C until analysis. Muscle extract was prepared essentially as previously described (30). Briefly, the tissue sample was extracted in SET buffer (250 mM Sucrose, 2 mM EDTA, 10 mM Tris, pH 7.4) in the presence of protease and phosphatase inhibitors (Complete and PhosStop; Roche) by homogenization and ultrasound treatment, followed by centrifugation. Supernatant was used for immunoprecipitation (see above) using the indicated antibodies.

Yeast two-hybrid (Y2H) analyses
Yeast two-hybrid analysis was performed as previously described (20, 24). Briefly, interaction analysis using yeast THY-AP4 strain (*MATa, ura3, leu2, lexA::lacZ::trp1, lexA::HIS3, lexA::ADE2*) co-transformed with the indicated combination of plasmids (see above). Transformants were grown in selective 4 % glucose synthetic complete medium lacking the corresponding supplements to maintain selection for plasmids. The strength of the interaction was determined by measuring β-galactosidase activity in permeabilized yeast cells and expressed in Miller units. In all Y2H analyses similar protein levels were obtained from the expression constructs, as verified in the crude extracts from the different yeast transformants.

Statistical analysis
All bar graph data are presented as mean ± S.E.M., unless otherwise stated. Statistical differences were evaluated using unpaired Student's *t* test and statistical analysis software Prism 4 (GraphPad Software, Inc.). P values equal to or less than 0.05 were considered statistically significant.

RESULTS

R6 preferentially interacts with AMPKβ2
We previously demonstrated that R6 (PPP1R3D), one of the glycogen-targeting subunits of the protein phosphatase 1 (PP1), physically interacts with AMPKβ1 in MIN6 pancreatic β cells (20). To verify AMPKβ1/R6 interaction in HEK293T cells, we overexpressed myc-tagged AMPK□□□□□□□□□□□□□ heterotrimers (myc-α1, β1-mCherry, γ1), together with FLAG-tagged R6 (FLAG-R6) or empty vector control (EV). Physical interaction between AMPKβ1 and R6 was assessed by immunoprecipitation (IP) of AMPK from cells that were routinely cultured under glucose-rich conditions (25 mM glucose) (Fig. 1A). Pull-down of myc-AMPKα1 resulted in co-immunoprecipitation of both mCherry-tagged AMPKβ1 (65 kD) and FLAG-tagged R6, indicating formation of the heterotrimeric AMPK complex and the interaction with R6 (Fig. 1A). As expected, FLAG-R6 signal was absent in cells transfected with EV. Next, we investigated the interaction between muscle-specific AMPKβ2 heterotrimers (myc-α1, β2-mCherry, γ1) and R6 (FLAG-R6) using co-transfection and immunoprecipitation in HEK293T. As both proteins co-immunoprecipitated, this data points to the occurrence of a physical interaction between R6 and AMPKβ2 (Fig. 1B). Interestingly, co-immunoprecipitation appeared stronger in the presence of the AMPKβ2 compared to β1. These data were further confirmed by yeast-two-hybrid (Y2H) analyses: in Fig. 1C it is shown that R6 binds to both AMPKβ1 and β2, while the interaction between AMPKβ2 and R6 is

significantly stronger than the one between AMPKβ1 and R6. Combined, these findings suggest that R6 prefers interaction with AMPKβ2 over AMPKβ1.

R6 interaction with AMPKβ2 requires its substrate-binding motif

Recently, a number of functionally distinct protein domains have been identified in the R6 glycogen-targeting subunit of PP1 (23). R6 is composed of domains that mediate binding to carbohydrates (via its CBM), binding to the PP1 catalytic subunit (PP1c; RVXF motif), and to the glycogen metabolism-related substrates of PP1 (via the highly conserved WDNND motif). To investigate whether and which of these motifs are involved in the interaction between the AMPKβ subunit and R6, we performed studies in HEK293T cells co-expressing AMPKβ2 complex (myc-α1, β2-mCherry, γ1) with FLAG-R6, the latter carrying various mutations corresponding to its protein motifs (23) (Fig. 2A, B). We again immunoprecipitated myc-AMPKα1 using a myc-directed antibody. Of note, endogenous R6 was not detected either in lysate or in immunoprecipitated material, thereby substantiating the need for FLAG-R6 overexpression to study the interaction between AMPKβ2 and R6 (Fig. 2B: EV condition). R6 carried various domain-specific mutations: in both R6-RARA and R6-RAHA mutants, the hydrophobic valine and phenylalanine residues within putative R6-RVXF motifs were substituted for alanine, allowing us to probe the role of the PP1-binding motif in AMPKβ2/R6-binding (Fig. 2B). R6-RARA, a mutant known to have lost its capacity to bind to endogenous PP1c but not to PP1-substrates (23), presented a similar AMPKβ2-binding profile compared to wild-type, non-mutated R6 (R6-WT; Fig. 2B; right panel). The R6-RAHA mutant that carried mutations in a domain close to the substrate-binding motif, however, had completely lost its ability to interact with AMPK (Fig. 2B; right panel). This data was reproduced in a reciprocal Y2H assay using AMPKβ2 as bait (Fig. 2C). Further, the substrate-binding motif (WDNND) was mutated to study its effect on AMPKβ2/R6 interaction. In one of the mutants, the two aspartate residues present within the WDNND motif were replaced by alanine (R6-WANNA mutant), whereas in the R6-WDNAD mutant, the second asparagine residue was replaced by alanine. Whereas the R6-WDNAD mutant was still capable of interacting with AMPKβ2, the WANNA mutation abolished AMPKβ2 binding (Fig. 2B right panel and 2C). In good agreement, Y2H analyses using AMPKβ1 or AMPKβ2 as bait confirmed that the binding of R6 to the AMPKβ subunits depended on the R6 substrate-binding motif being intact (Fig. 2C and 2D). Thus, we show that the AMPKβ/R6 interaction requires the R6 substrate-binding motif. In all subsequent experiments, we concentrated on AMPKβ2/R6 interaction.

AMPKβ2 Thr-148 mutant shows reduced interaction with R6

Previously, we showed that substitution of the glycine-147 residue for arginine (G147R) within the β1-CBM domain abolished the interaction of AMPK with R6 (20), indicating that AMPKβ1 requires the CBM for interaction with R6. More recently, we demonstrated that autophosphorylation at the β-threonine-148 (Thr-148) residue, centrally located in the CBM, prevents AMPK from binding to carbohydrates such as glycogen (22). As we show here that R6 also interacts with AMPKβ2, we next investigated whether Thr-148 is required for AMPKβ2/R6 interaction. To this end, a phospho-mimicking AMPKβ2 mutant was generated by substituting the threonine-148 residue for aspartate (T148D) within the β2-CBM. Transiently transfected HEK293T cells co-expressing FLAG-R6 and AMPK heterotrimers (myc-α1 and γ1 in combination with either β2-WT- or β2-T148D-mCherry), were cultured under high glucose conditions (25 mM) and used for co-immunoprecipitation analysis. Impaired interaction between AMPKβ2 and R6 was observed in cells overexpressing mutant AMPKβ2-T148D (Fig. 3A; right panel); relevantly, FLAG-R6 and mCherry-β2 were expressed at comparable levels (Fig. 3A; left panel). Independent Y2H analyses corroborated these findings: T148D mutation decreased the interaction between AMPKβ2 and R6 (Fig. 3B). Taken together, our data indicate that Thr-148 mutation into aspartate results in loss of AMPKβ2/R6 interaction, suggesting that an intact Thr-148 residue is essential for the formation of the AMPKβ2/R6 complex under glucose-rich culturing conditions.

Glycogen depletion enhances the interaction between AMPKβ2 and R6

To investigate whether the interaction between AMPKβ2 and R6 is responsive to variation in glycogen level, we aimed to deplete cellular glycogen content. Hence, HEK293T cells were either pharmacologically treated with forskolin, a compound inducing glycogen breakdown (31), or glucose-deprived, after which glycogen content was assessed. Because R6 is known to have glycogenic properties (24), we included non-transfected control cells and compared these with cells that were either transfected with FLAG-R6 alone, or co-transfected with all three subunits of AMPK (myc-α1, β2-WT-mCherry, γ1). As expected, cells overexpressing FLAG-R6 showed high glycogen content (both in the absence and presence of overexpressed AMPKβ2 complex): basal glycogen levels were 30 − 40-fold increased compared to non-transfected control cells (Fig. 4A). Both forskolin-treatment and glucose-deprivation significantly lowered the intracellular glycogen levels in all cell lines, as compared to control (Fig. 4A). To assess the effect of cellular glycogen content on AMPKβ2/R6 interaction, HEK293T cells overexpressing both FLAG-R6 and AMPKβ2 heterotrimers were either treated with forskolin or glucose-deprived for 16 h. Reduction of cellular glycogen content, either by forskolin-treatment or glucose-deprivation, substantially enhanced the interaction between AMPKβ2 and R6 that was accompanied by a similar increase in the T172 phosphorylation level (Fig. 4B; right panel); as total levels of AMPK and R6 did not change within the experimental time frame (Fig. 4B; left panel), this ruled out any possible interference by altered expression. Further, we examined whether the binding of overexpressed AMPKβ2 to FLAG-R6 is reversible (Fig. 4C). Expectedly, immunoprecipitates of AMPK from cells that were cultured in low glucose medium displayed clear interaction with R6. When cells were switched back to incubation in high glucose medium this association decreased time-dependently resulting in a complete loss of the AMPKβ2/R6 interaction after 30 minutes. Collectively, our data suggest that the interaction between AMPKβ2 heterotrimers and R6 is dynamic and inversely correlated to cellular glycogen level.

To independently examine a possible direct effect of glycogen on the AMPKβ2/R6 binding, we next used β-cyclodextrin (β-CD), a model-sugar that mimics glycogen, in competitive binding-immunoprecipitation experiments in HEK293T cells cultured under high glucose. Addition of β-CD completely disrupted the interaction between AMPKβ2 and R6 (Fig. 4D; right panel). Combined, these data suggest that under glucose-rich conditions glycogen disturbs AMPKβ2/R6 interaction, indicating that glycogen interferes with and therefore weakens the interaction between AMPKβ2 and R6.

AMPKβ2/R6 interaction is enhanced by glycogen depletion in conjunction with increased AMPKβ2 Thr-148 phosphorylation

Next, we assessed the impact of Thr-148 phosphorylation on the glycogen-modulated AMPKβ2/R6 interaction. To this end, we co-transfected HEK293T cells with AMPK heterotrimers (myc-α1, γ1, and either mCherry-tagged β2-WT or -T148D mutant) and FLAG-R6, and challenged the cells for 16 h with various concentrations of glucose. The expression of AMPKβ2-T148D mutant did not affect the glycogenic activity of FLAG-R6 in cells cultured under high glucose conditions (Fig. 5A), indicating that glycogen production depends on the function of R6 but not on the interaction between R6 and AMPKβ2. Reduced availability of glucose (*i.e.*, 3 mM or 0 mM) correlated with significantly decreased intracellular levels of glycogen in both AMPKβ2-WT and -T148D expressing cells (Fig. 5A). Interestingly, we observed increased levels of Thr-148 phosphorylation in β2-WT immunoprecipitates upon lowering glucose conditions, although we did not find changes in the levels of AMPK Thr-172 phosphorylation, neither in cellular lysates nor in the precipitates from β2-WT or β2-T148D expressing cells (Fig. 5B). Low glycogen content enhanced AMPKβ2/R6 interaction (Fig. 5B; *cf.* Fig. 4). Whereas AMPKβ2-WT/R6 binding was readily detectable, T148D mutation completely abolished AMPKβ2 interaction with R6, independent of the glycogen status (Fig. 5B; *cf.* Fig. 3). Further, we investigated the effect of AMPK activation on AMPKβ2/R6 interaction using various AMPK activating stimuli (Fig. 5C). Again, AMPKβ2-T148D mutant did not associate with R6 in any of the conditions tested. AMPK activation generally enhanced AMPKβ2-WT/R6 interaction. Oligomycin exhibited the strongest AMPK activating effect (Thr-172 phosphorylation in Fig. 5C; left panel). AMPKβ2 Thr-148 phosphorylation and the binding of R6 to AMPKβ2 were greatly enhanced by oligomycin (Fig. 5C; right panel). Next, we exposed

cells to oligomycin in the context of high and low cellular glycogen. If glycogen content was low (*i.e.,* 3 mM glucose), oligomycin activated AMPK (Thr-172 phosphorylation; Fig. 5D), an effect that was overruled by high cellular glycogen content (*i.e.,* 25 mM glucose). Oligomycin-induced activation of AMPK and the consequential Thr-148 phosphorylation further enhanced the interaction of AMPKβ2-WT and R6 (Fig. 5D; right panel) under low glycogen conditions. This interaction was disrupted by high cellular glycogen or by T148D mutation (Fig. 5D). These results indicate that glycogen-depletion enhances both AMPKβ2/R6 interaction and phosphorylation of Thr-148. Our data also indicate that phosphorylation of AMPKβ2 at Thr-148 has a different outcome from AMPKβ2-T148D mutant: whereas the AMPKβ2-T148D mutant is not able to interact with R6, AMPKβ2/R6 interaction is improved under conditions that enhance AMPKβ2 Thr-148 phosphorylation.

Endogenous AMPKβ2 shows enhanced interaction with R6 upon glycogen depletion in C2C12 myotubes

Furthermore, we explored the significance of cellular glycogen with respect to AMPKβ2/R6 interaction in C2C12 myotubes, a more physiologically relevant model. Similar to all other tested cell types, endogenous R6 was below detection level in C2C12 cells using a variety of available antibodies (data not shown). Hence, we stably expressed FLAG-R6 or empty vector (EV) control in C2C12 myoblasts. C2C12 cells were then differentiated to myotubes and cultured under high (*i.e.*, 25 mM) or low (*i.e.*, 3 mM) glucose concentrations prior to oligomycin-treatment. We determined glycogen content and AMPKβ2/R6 interaction for each condition (Fig. 6A, B). Both lowered glucose availability and oligomycin-treatment reduced the myocellular glycogen content below detection level in cells expressing the EV control (Fig. 6A). R6 overexpression greatly enhanced the levels of glycogen under basal and treated conditions (Fig. 6A). Oligomycin challenged the glycogen levels (Fig, 6A) and clearly induced AMPK activation in C2C12 myotubes, under both high and low glucose conditions (Fig 6B, left panel). However, as in HEK293T cells, oligomycin-mediated AMPK activation could only be detected in immunoprecipitates from cells that were cultured under low glycogen conditions (Fig. 6B; right panel). As expected, increased interaction of AMPKβ2 with R6 was detected after immunoprecipitating FLAG-R6 from oligomycin-treated cells under low glycogen conditions (Fig. 6B; right panel). By performing the reverse immunoprecipitation using AMPKα1/α2-directed antibodies, we also detected enhanced FLAG-R6 presence in the low glycogen condition (Fig. 6C). Moreover, we detected T148-phosphorylation of endogenous AMPKβ2, which expectedly was highest in conjunction with low glycogen in oligomycin-treated immunoprecipitates (Fig. 6C). We further assessed the presence of Thr-148 phosphorylation in a physiological context. Gastrocnemius muscle was obtained from untreated mice and AMPK was immunoprecipitated from homogenates (Fig. 6D). As shown by Western blotting, Thr-148 phosphorylation signal was evident. Decrease of this signal upon incubation with calf intestine phosphatase (CIP) further confirms the phosphorylation event. Therefore, skeletal muscle may operate signaling pathways involving phosphorylated Thr-148. Taken together, in good agreement with our observations in HEKT293 cells, the data obtained from C2C12 myotubes support the notion that cellular glycogen content controls AMPKβ2/R6 binding. Also, Thr-148 phosphorylation of endogenous AMPKβ2 occurred in conjunction with R6 interaction in C2C12 myotubes

AMPKβ2 Thr-148 mutant enhances glycogen content of C2C12 myotubes

We next studied the effect of expressing AMPKβ2-T148D mutant in C2C12 cells in terms of glucose uptake and glycogen accumulation. To this end, we stably expressed AMPKβ2-WT or -T148D mutant in C2C12 cells, and after differentiation, cells were incubated in high, low or absence of glucose. Expectedly, the glycogen levels were challenged by low or no glucose incubations (Fig. 7A). However, relative to WT, the T148D mutant overexpressing cells showed higher glycogen content (under high glucose). Since AMPKβ2-T148D mutant does not associate with glycogen (and R6), these data could indicate a function of the AMPKβ2-T148D mutant that is independent of the glycogen particle, possibly by improving glucose uptake. However, glucose uptake changes were statistically insignificant (Fig. 7B).

DISCUSSION

In the current study, we demonstrate the involvement of Thr-148 in the dynamic AMPKβ2/R6 interaction that is governed by glycogen content.

Due to the positioning of Thr-148 in the carbohydrate-binding pocket, the phosphorylation of this residue is incompatible with glycogen binding Glucose deprivation expectedly resulted in reduced glycogen levels (Figs. 4-7). Accordingly, we detected strong AMPKβ2 Thr-148 phosphorylation signals only when glycogen levels were low, which were further augmented by oligomycin treatment (Fig. 5). Similar to GS, which dissociates from glycogen in response to glycogen breakdown (32, 33), decreased glycogen content may also cause AMPKβ2 and R6 to leave glycogen. In support of such notion, oligomycin-induced AMPK activation augmented AMPKβ2/R6 interaction also in C2C12 myotubes, while further depleting glycogen and inducing Thr-148 phosphorylation (Fig. 6), strongly suggesting that these events are linked. In conjunction with lowered glycogen content, oligomycin-induced Thr-172 phosphorylation was also more effective, which ties in with autophosphorylation of Thr-148, *i.e.*, by AMPK. Thus, autophosphorylation of Thr-148 by AMPK may indicate detachment of AMPK from glycogen in conditions that challenge the cellular glycogen level.

We find that phosphorylation of AMPKβ2 at Thr-148 enhanced the binding to R6, whereas AMPKβ2/R6 interaction was completely lost in the AMPKβ2-T148D mutant. The latter results are in agreement with earlier observations, where the AMPKβ1-G147R mutation impaired the ability to interact with R6 (20). Since AMPKβ Thr-148 is located adjacent to Gly-147, a similar loss of binding to R6 for the Thr-148 mutant was expected. Nevertheless, the molecular mechanism explaining the loss of binding to R6 as a result of T148D mutation remains unclear, because Thr-148 phosphorylation was enhanced in conjunction with AMPKβ2/R6 interaction (Fig. 5). In our previous study, we found that T148D mutant did not bind glycogen (22). Hence, there are at least two possible explanations: (*i*) the T148D mutation causes a subtle modification in the conformation of the β2 subunit resulting in the loss of interaction with R6, a process not shared by the physiological phosphorylation of this subunit; or (*ii*) the interaction of AMPKβ2-WT with R6 that is observed during glycogen degradation evolves from their initial binding at glycogen. These explanations are not mutually exclusive and we formally cannot rule out the former, but there are arguments in support of the latter notion. Firstly, both AMPKβ2 and R6 bind to glycogen via their respective CBM (12, 34). The co-localization of AMPK and R6 to glycogen brings them in close proximity to each other, which may facilitate their subsequent direct interaction, i.e., as a second step during conditions that degrade glycogen. Hence, the possible mechanisms causing AMPKβ2 and R6 to leave the dwindling glycogen particle may include the decreasing surface binding options. On a diminishing glycogen granule, we can indeed expect the concentration of potential interaction partners to increase dramatically, which may facilitate a direct binding between these proteins concomitant with their detachment from glycogen. This is in accordance with our findings showing that depletion of intracellular glycogen resulted in enhanced AMPKβ2/R6 interaction (Figs. 4-6). In particular, the AMPKβ2/R6 complex was more abundant in glucose-deprived or forskolin-treated cells (Fig. 4B). Similarly, in earlier Y2H analyses, low glucose media augmented the AMPKβ1/R6 interaction (35). Secondly, high glycogen content was found to decrease AMPKβ2/R6 interaction (Figs. 4-6), and thus glycogen may in fact rather perturb the direct binding between AMPKβ2 and R6. In addition, AMPKβ2/R6 binding decreased upon treatment of co-immunoprecipitations with β-CD (Fig. 4D). Since the R6-substrate-binding motif partially overlaps with the CBM domain (23), it is conceivable that glycogen competes with R6 binding to AMPK. Thus, our data suggest that low glycogen favors AMPKβ2/R6 interaction, whereas high glycogen content interferes with it. We propose that the AMPKβ2-T148D mutant, due to lack of glycogen-binding affinity, is excluded from the interaction with R6 because this process initiates at glycogen.

AMPK plays an essential role in various biological processes involved in restoring cellular energy homeostasis. Tuning of such processes requires adequate regulation, and involves AMPK compartmentalization and complex formation with other proteins and substrates. In the present study, we show that R6 preferentially interacts with AMPKβ2, rather than AMPKβ1, pointing to a possible role for this interaction in skeletal muscle. The CBM domain of AMPKβ2 possesses higher binding affinity for

carbohydrates such as glycogen than β1 (14). In a more detailed study the CBM domain of AMPKβ2 bound linear carbohydrates and single α1,6-branched carbohydrates 4-30 fold tighter in comparison with β1 (36). AMPKβ2, as well as R6, are highly expressed in skeletal muscle (3, 37), a tissue active in controlling disposal of glucose into glycogen (38). Thus, it is likely that these proteins contribute to the regulation of myocellular glycogen turnover. Recent *in vivo* studies seemingly contradict the importance of AMPKβ2 in glycogen metabolism: The observed differences in glycogen content were marginal between WT and AMPKβ1/β2 double knockout mice pre- and post-exercise (39). In AMPKβ2 knockout mice, muscular glycogen content was reduced pre-exercise and was equal with a slight tendency to increase post-exercise (6, 7). However, since there is a reduction in the levels of skeletal muscle AMPKα1 and α2 in β2 knockout mice and a dramatic reduction of the levels of the AMPK complex subunits in double AMPKβ1/β2 knockout mice, it is difficult to make any correlation between the levels of glycogen in these mice and the activity of AMPK. We recently showed that activation of AMPK precedes AMPKβ Thr-148 autophosphorylation to preclude the AMPK complex from binding to glycogen and further data suggested a possible role for Thr-148 phosphorylation in glycogen turnover in several cell lines (22). Thus, independent of possible functions for AMPK complexes that are bound at glycogen particles, free cytosolic AMPK may also indirectly affect glycogen metabolism, as further supported by T148D overexpression in C2C12 myotubes (Figure 7). Moreover, R6 is a known glycogen-binding protein and PP1-targeting subunit acting as a glycogenic driver (24). Hence, it is conceivable to expect that AMPKβ2/R6 interaction is playing an important role in glycogen metabolism in muscle.

In yeast, it was reported earlier that Gal83 (Snf1 β-subunit ortholog) is involved in binding to Reg1 (PP1 glycogenic subunit ortholog) and studies in mouse pancreatic β cells revealed that AMPKβ1 interacts with the PP1-glycogen targeting subunit R6 (20, 40). R6 recruits PP1 phosphatase to its substrates (*e.g.,* GS and GP) (23), thus playing a critical role in the regulation of glycogen metabolism. Most of the PP1-glycogen-targeting subunits exert their actions through binding to PP1 via a conserved N-terminal PP1-binding motif (RVXF), and interact with PP1-substrates via a conserved C-terminal substrate-binding (WXNXGNYX(L/I)) motif (23). We have recently shown that R6 utilizes this conserved region to bind to its glycogenic substrates GS and GP (23). In line with these results, our work indicates that AMPKβ/R6 interaction occurs also via the R6 substrate-binding motif (Fig. 2), as a mutation in this domain resulted in loss of interaction, a process that is independent of PP1 binding. However, we did not find evidence for R6/PP1-dependent AMPK dephosphorylation in our study under conditions where AMPKβ2/R6 interaction was enhanced. This may be attributed to the use of glycogen depletion and mitochondrial poisoning as triggers. Although we find these treatments as required to induce significant AMPKβ2/R6 interaction, their application necessarily goes along with elevated AMP levels and consequent protection from Thr-172 dephosphorylation (41). In MIN6 pancreatic β-cells, the R6/PP1 complex was responsible for AMPK dephosphorylation at Thr-172 in response to high extracellular glucose (20). In HEK293 cells, we find that glucose re-availability leads to a transient decrease of Thr-172 phosphorylation (Fig. 4C). In the same experiment, AMPKβ2/R6 interaction disappeared time-dependently after recovery with high glucose. Hence, the idea that R6 could act as a scaffold to bring AMPKβ2 in close proximity to the PP1 phosphatase warrants further investigation. The present data establish that AMPKβ2/R6 complex formation and dissociation are reversible and dynamic processes that involve the substrate-binding site of R6. Taken together, we shed new light on the molecular events that govern the interaction of AMPK with R6.

ACKNOWLEDGMENTS

We thank the members of the Molecular Genetics department of Maastricht University for helpful comments and support.

DECLARATIONS OF INTEREST

The authors declare that they have no conflicts of interest with the contents of this article.

AUTHOR CONTRIBUTIONS

Yvonne Oligschlaeger, Marie Miglianico, Vivian Dahlmans, Carla Rubio-Villena, Dipanjan Chanda, Maria Adelaida Garcia-Gimeno, Will Coumans, Yilin Liu, Pascual Sanz and Dietbert Neumann designed and carried out the experiments. Yvonne Oligschlaeger, Pascual Sanz and Dietbert Neumann wrote the manuscript. Jan Willem Voncken, Joost Luiken and Jan Glatz contributed with material, provided conceptual input and assisted in the manuscript preparation. All authors reviewed the results and approved the final version of the manuscript.

FUNDING

DN is recipient of a VIDI-Innovational Research Grant from the Netherlands Organization of Scientific Research (NWO-ALW Grant no. 864.10.007). This work has further been supported by grants from the Spanish Ministry of Education and Science SAF2014-54604-C3-1-R and a grant from Generalitat Valenciana (PrometeoII/2014/029) to PS.

REFERENCES

1. Jornayvaz FR, Samuel VT, Shulman GI. The role of muscle insulin resistance in the pathogenesis of atherogenic dyslipidemia and nonalcoholic fatty liver disease associated with the metabolic syndrome. Annu Rev Nutr. 2010;30:273-90.
2. Kurth-Kraczek EJ, Hirshman MF, Goodyear LJ, Winder WW. 5' AMP-activated protein kinase activation causes GLUT4 translocation in skeletal muscle. Diabetes. 1999;48(8):1667-71.
3. Thornton C, Snowden MA, Carling D. Identification of a novel AMP-activated protein kinase beta subunit isoform that is highly expressed in skeletal muscle. J Biol Chem. 1998;273(20):12443-50.
4. Chen Z, Heierhorst J, Mann RJ, Mitchelhill KI, Michell BJ, Witters LA, et al. Expression of the AMP-activated protein kinase beta1 and beta2 subunits in skeletal muscle. FEBS Lett. 1999;460(2):343-8.
5. Dzamko N, van Denderen BJ, Hevener AL, Jorgensen SB, Honeyman J, Galic S, et al. AMPK beta1 deletion reduces appetite, preventing obesity and hepatic insulin resistance. J Biol Chem. 2010;285(1):115-22.
6. Dasgupta B, Ju JS, Sasaki Y, Liu X, Jung SR, Higashida K, et al. The AMPK beta2 subunit is required for energy homeostasis during metabolic stress. Mol Cell Biol. 2012;32(14):2837-48.
7. Steinberg GR, O'Neill HM, Dzamko NL, Galic S, Naim T, Koopman R, et al. Whole body deletion of AMP-activated protein kinase {beta}2 reduces muscle AMPK activity and exercise capacity. J Biol Chem. 2010;285(48):37198-209.
8. McGee SL, Howlett KF, Starkie RL, Cameron-Smith D, Kemp BE, Hargreaves M. Exercise increases nuclear AMPK alpha2 in human skeletal muscle. Diabetes. 2003;52(4):926-8.
9. Kodiha M, Rassi JG, Brown CM, Stochaj U. Localization of AMP kinase is regulated by stress, cell density, and signaling through the MEK-->ERK1/2 pathway. Am J Physiol Cell Physiol. 2007;293(5):C1427-36.
10. Carling D, Clarke PR, Zammit VA, Hardie DG. Purification and characterization of the AMP-activated protein kinase. Copurification of acetyl-CoA carboxylase kinase and 3-hydroxy-3-methylglutaryl-CoA reductase kinase activities. Eur J Biochem. 1989;186(1-2):129-36.
11. Kazgan N, Williams T, Forsberg LJ, Brenman JE. Identification of a nuclear export signal in the catalytic subunit of AMP-activated protein kinase. Mol Biol Cell. 2010;21(19):3433-42.
12. Polekhina G, Gupta A, Michell BJ, van Denderen B, Murthy S, Feil SC, et al. AMPK β Subunit Targets Metabolic Stress Sensing to Glycogen. Current Biology. 2003;13(10):867-71.
13. Hudson ER, Pan DA, James J, Lucocq JM, Hawley SA, Green KA, et al. A Novel Domain in AMP-Activated Protein Kinase Causes Glycogen Storage Bodies Similar to Those Seen in Hereditary Cardiac Arrhythmias. Current Biology. 2003;13(10):861-6.
14. Koay A, Woodcroft B, Petrie EJ, Yue H, Emanuelle S, Bieri M, et al. AMPK beta subunits display isoform specific affinities for carbohydrates. FEBS Lett. 2010;584(15):3499-503.

15. Wojtaszewski JF, Jorgensen SB, Hellsten Y, Hardie DG, Richter EA. Glycogen-dependent effects of 5-aminoimidazole-4-carboxamide (AICA)-riboside on AMP-activated protein kinase and glycogen synthase activities in rat skeletal muscle. Diabetes. 2002;51(2):284-92.
16. Hunter RW, Treebak JT, Wojtaszewski JF, Sakamoto K. Molecular mechanism by which AMP-activated protein kinase activation promotes glycogen accumulation in muscle. Diabetes. 2011;60(3):766-74.
17. Fong NM, Jensen TC, Shah AS, Parekh NN, Saltiel AR, Brady MJ. Identification of binding sites on protein targeting to glycogen for enzymes of glycogen metabolism. J Biol Chem. 2000;275(45):35034-9.
18. Heroes E, Lesage B, Gornemann J, Beullens M, Van Meervelt L, Bollen M. The PP1 binding code: a molecular-lego strategy that governs specificity. FEBS J. 2013;280(2):584-95.
19. Armstrong CG, Browne GJ, Cohen P, Cohen PTW. PPP1R6, a novel member of the family of glycogen-targetting subunits of protein phosphatase 1. FEBS Letters. 1997;418(1-2):210-4.
20. Garcia-Haro L, Garcia-Gimeno MA, Neumann D, Beullens M, Bollen M, Sanz P. The PP1-R6 protein phosphatase holoenzyme is involved in the glucose-induced dephosphorylation and inactivation of AMP-activated protein kinase, a key regulator of insulin secretion, in MIN6 beta cells. FASEB J. 2010;24(12):5080-91.
21. Sanz P, Alms GR, Haystead TA, Carlson M. Regulatory interactions between the Reg1-Glc7 protein phosphatase and the Snf1 protein kinase. Mol Cell Biol. 2000;20(4):1321-8.
22. Oligschlaeger Y, Miglianico M, Chanda D, Scholz R, Thali RF, Tuerk R, et al. The Recruitment of AMP-activated Protein Kinase to Glycogen Is Regulated by Autophosphorylation. J Biol Chem. 2015;290(18):11715-28.
23. Rubio-Villena C, Sanz P, Garcia-Gimeno MA. Structure-Function Analysis of PPP1R3D, a Protein Phosphatase 1 Targeting Subunit, Reveals a Binding Motif for 14-3-3 Proteins which Regulates its Glycogenic Properties. PLoS One. 2015;10(6):e0131476.
24. Rubio-Villena C, Garcia-Gimeno MA, Sanz P. Glycogenic activity of R6, a protein phosphatase 1 regulatory subunit, is modulated by the laforin-malin complex. Int J Biochem Cell Biol. 2013;45(7):1479-88.
25. Gimeno-Alcaniz JV, Sanz P. Glucose and type 2A protein phosphatase regulate the interaction between catalytic and regulatory subunits of AMP-activated protein kinase. J Mol Biol. 2003;333(1):201-9.
26. Kinsella TM, Nolan GP. Episomal vectors rapidly and stably produce high-titer recombinant retrovirus. Hum Gene Ther. 1996;7(12):1405-13.
27. Morgenstern JP, Land H. Advanced mammalian gene transfer: high titre retroviral vectors with multiple drug selection markers and a complementary helper-free packaging cell line. Nucleic Acids Res. 1990;18(12):3587-96.
28. Voncken JW, Niessen H, Neufeld B, Rennefahrt U, Dahlmans V, Kubben N, et al. MAPKAP kinase 3pK phosphorylates and regulates chromatin association of the polycomb group protein Bmi1. J Biol Chem. 2005;280(7):5178-87.
29. Schwenk RW, Dirkx E, Coumans WA, Bonen A, Klip A, Glatz JF, et al. Requirement for distinct vesicle-associated membrane proteins in insulin- and AMP-activated protein kinase (AMPK)-induced translocation of GLUT4 and CD36 in cultured cardiomyocytes. Diabetologia. 2010;53(10):2209-19.
30. Skehel JM. Preparation of extracts from animal tissues. Methods Mol Biol. 2004;244:15-20.
31. Singh PK, Singh S, Ganesh S. The laforin-malin complex negatively regulates glycogen synthesis by modulating cellular glucose uptake via glucose transporters. Mol Cell Biol. 2012;32(3):652-63.
32. Nielsen JN, Derave W, Kristiansen S, Ralston E, Ploug T, Richter EA. Glycogen synthase localization and activity in rat skeletal muscle is strongly dependent on glycogen content. J Physiol. 2001;531(Pt 3):757-69.
33. Prats C, Cadefau JA, Cusso R, Qvortrup K, Nielsen JN, Wojtaszewski JF, et al. Phosphorylation-dependent translocation of glycogen synthase to a novel structure during glycogen resynthesis. J Biol Chem. 2005;280(24):23165-72.

34. Machovic M, Janecek S. Starch-binding domains in the post-genome era. Cell Mol Life Sci. 2006;63(23):2710-24.
35. Garcia-Haro L, Garcia-Gimeno MA, Neumann D, Beullens M, Bollen M, Sanz P. Glucose-dependent regulation of AMP-activated protein kinase in MIN6 beta cells is not affected by the protein kinase A pathway. FEBS Lett. 2012;586(23):4241-7.
36. Mobbs JI, Koay A, Di Paolo A, Bieri M, Petrie EJ, Gorman MA, et al. Determinants of oligosaccharide specificity of the carbohydrate-binding modules of AMP-activated protein kinase. Biochem J. 2015;468(2):245-57.
37. Montori-Grau M, Guitart M, Garcia-Martinez C, Orozco A, Gomez-Foix AM. Differential pattern of glycogen accumulation after protein phosphatase 1 glycogen-targeting subunit PPP1R6 overexpression, compared to PPP1R3C and PPP1R3A, in skeletal muscle cells. BMC Biochem. 2011;12:57.
38. Ren JM, Marshall BA, Gulve EA, Gao J, Johnson DW, Holloszy JO, et al. Evidence from transgenic mice that glucose transport is rate-limiting for glycogen deposition and glycolysis in skeletal muscle. J Biol Chem. 1993;268(22):16113-5.
39. O'Neill HM, Maarbjerg SJ, Crane JD, Jeppesen J, Jorgensen SB, Schertzer JD, et al. AMP-activated protein kinase (AMPK) beta1beta2 muscle null mice reveal an essential role for AMPK in maintaining mitochondrial content and glucose uptake during exercise. Proc Natl Acad Sci U S A. 2011;108(38):16092-7.
40. Mangat S, Chandrashekarappa D, McCartney RR, Elbing K, Schmidt MC. Differential roles of the glycogen-binding domains of beta subunits in regulation of the Snf1 kinase complex. Eukaryot Cell. 2010;9(1):173-83.
41. Suter M, Riek U, Tuerk R, Schlattner U, Wallimann T, Neumann D. Dissecting the role of 5'-AMP for allosteric stimulation, activation, and deactivation of AMP-activated protein kinase. J Biol Chem. 2006;281(43):32207-16.

FIGURE LEGENDS

Figure 1. R6 preferentially interacts with AMPKβ2
(A and **B)** HEK293T cells transiently overexpressing FLAG-R6 and heterotrimers of AMPKβ1 (myc-α1, γ1, AMPKβ1-mCherry) **(A)** or AMPKβ2 (myc-α1, γ1, AMPKβ2-mCherry) **(B)**. FLAG empty vector (EV) was used as control. Cells were continuously cultured under high glucose (25 mM) conditions and harvested 56 h post-transfection. Interaction between AMPKβ1/2 and R6 was assessed by immunoprecipitating the heterotrimeric AMPK complex from 800 μg of lysate using the anti-myc-tag antibody. Western blots were assessed using the indicated antibodies. Representative Western blots are shown. **(C)** Yeast THY-AP4 strain (see Materials and Methods) was transformed with the indicated combination of plasmids. Transformants were grown in high glucose (4 % glucose) containing medium and protein interactions were estimated by measuring the β-galactosidase activity. Empty vector pGADT7 (GAD-Φ) served as control. Values correspond to means from at least 6 different transformants (bars indicate S.D.). * $p<0.001$ *vs.* LexA-AMPKβ1-WT + GAD-R6.

Figure 2. R6 interaction with AMPKβ2 requires its substrate-binding motif
(A) Schematic model indicating the PP1- and substrate-binding sites of R6, and its corresponding mutations. **(B)** HEK293T cells transiently co-expressing AMPKβ2 heterotrimers (myc-α1, γ1, AMPKβ2-mCherry) and FLAG-R6 wild-type (R6-WT) or mutant (R6-RARA, R6-RAHA, R6-WANNA, R6-WDNAD, respectively) were continuously cultured under high glucose (25 mM) conditions and harvested 48 h post-transfection. FLAG empty vector (EV) was used as control. Interaction between AMPKβ2 and R6 was assessed by immunoprecipitating the heterotrimeric AMPK complex from 450 μg of lysate using the anti-myc-tag antibody. Western blots were assessed using the indicated antibodies. Representative Western blots are shown. **(C** and **D)** Yeast THY-AP4 strain (see Materials and Methods) was transformed with GAD-AMPKβ2 (**C**) or GAD-AMPKβ1 (**D**) plasmids and LexA-R6 plasmids as indicated. Transformants were grown in high glucose (4 % glucose) containing medium and protein interactions were estimated by measuring the β-galactosidase activity. Values correspond to means from at least 6 different transformants (bars indicate S.D.). * $p<0.05$ and ** $p<0.001$ *vs.* LexA-R6-WT.

Figure 3. AMPKβ2 Thr-148 mutant shows reduced interaction with R6
(A) HEK293T cells transiently transfected with myc-α1, γ1 and mCherry-tagged AMPKβ2 wild-type (WT) or Thr-148 mutant (T148D) were co-transfected either with FLAG-R6 (+), or FLAG empty vector (-) as control. Cells were cultured under high glucose (25 mM) conditions, and harvested 56 h post-transfection. Interaction between AMPKβ2 and R6 was assessed by immunoprecipitating the heterotrimeric AMPK complex from 800 μg of lysate using the anti-myc-tag antibody. Western blots were assessed using the indicated antibodies. Representative Western blots are shown. **(B)** Yeast THY-AP4 strain was transformed with plasmids LexA-AMPKβ2-WT or LexA-AMPKβ2-T148D and GAD-R6 as indicated. Transformants were grown in high glucose (4 % glucose) containing medium and protein interactions were estimated by measuring the β-Galactosidase activity. Empty vector pGADT7 (GAD-Φ) served as control. Values correspond to means from at least 6 different transformants (bars indicate S.D.). * $p<0.001$ *vs.* LexA-AMPKβ2-WT + GAD-R6.

Figure 4. Glycogen depletion enhances the interaction between AMPKβ2 and R6
(A and **B)** HEK293T cells either non-transfected, transiently transfected with FLAG-R6 alone, or co-transfected with FLAG-R6, myc-α1, γ1 and mCherry-tagged AMPKβ2-WT were cultured under high glucose (25 mM) conditions. Prior to lysis, cells were treated with forskolin (100 μM) or DMSO (control) under high glucose conditions, or cells were glucose-deprived (GD, 0 mM) for 16 h. **(A)** Intracellular glycogen level was determined as described in the section Materials and Methods. Levels were corrected for corresponding protein concentrations. * $p<0.05$ *vs.* corresponding DMSO controls; $n=2$. **(B)** Heterotrimeric AMPK was immunoprecipitated from 500 μg of lysate using the anti-myc-tag antibody, followed by Western blot analysis using the indicated antibodies. **(C)** HEK293T cells transiently

transfected with FLAG-R6, myc-α1, γ1 and mCherry-tagged AMPKβ2-WT were cultured under low glucose (3 mM) conditions and recovered with high glucose medium for the indicated time period before lysis and immunoprecipation. **(D)** HEK293T cells were transiently co-transfected as indicated and harvested 56 h post-transfection. Cells were continuously grown under high glucose (25 mM) conditions. β-Cyclodextrin (β-CD; 5 mM) was added prior to immunoprecipitation. Representative Western blots are shown.

Figure 5. AMPKβ2/R6 interaction is enhanced in conjunction with increased AMPKβ2 Thr-148 phosphorylation

HEK293T cells were transiently transfected for co-expression of AMPKβ2 heterotrimers (myc-α1, γ1, mCherry-tagged AMPKβ2-WT or -T148D) and FLAG-R6. **(A** and **B)** Prior to lysis, cells were cultured under various glucose conditions (*i.e.*, 25 mM, 3 mM, 0 mM) for 16 h. **(A)** Intracellular glycogen levels were biochemically determined and corrected for the corresponding protein concentrations. * $p<0.01$ *vs.* WT 25 mM, # $p<0.01$ *vs.* T148D 25 mM, ## $p<0.001$ *vs.* T148D 25 mM; $n=2$. **(B)** Heterotrimeric AMPK was immunoprecipitated from 350 μg of lysate using the anti-myc-tag antibody, followed by Western blot analysis using the indicated antibodies. **(C)** Cells were either maintained in growth medium (GM) or serum- starved (5.5 mM glucose) for 16 h and treated with vehicle (DMSO) or a variety of AMPK activators for 1 h as indicated. AMPK complexes were immunoprecipitated from 350 μg of lysate using the anti-myc-tag antibody, followed by Western blot analysis using various antibodies. **(D)** Cells were serum-starved both under low (3 mM) and high (25 mM) glucose conditions for 16 h, prior to 1 h treatment with oligomycin (3 μM) or DMSO (control). AMPK was immunoprecipitated from 500 μg of lysate as described in panel B, followed by Western blot analysis using the indicated antibodies. Representative Western blots are shown.

Figure 6. Endogenous AMPKβ2 shows enhanced interaction with R6 upon glycogen depletion in C2C12 myotubes

C2C12 cells stably overexpressing FLAG-R6 were differentiated into myotubes for 4-5 days, and subsequently incubated with high (25 mM) or low (3 mM) glucose for 16 h, followed by 30 minutes treatment with oligomycin (5 μM) or DMSO (control). pBabe-puromycin empty vector (EV) was used as control. **(A)** Myocellular glycogen levels were determined using biochemical glycogen assay, as described in Materials and Methods. * $p<0.05$, ** $p<0.01$, *** $p<0.001$; $n=3$. (**B**) Interaction between AMPKβ2 and R6 was assessed by immunoprecipitation using the anti-FLAG-tag antibody, followed by Western blot analysis using the indicated antibodies. **(C)** Interaction between AMPKβ2 and R6 was assessed by immunoprecipitation using anti-AMPKα1/α2 antibodies, followed by Western blot analysis using the indicated antibodies. **(D)** Mouse gastrocnemius muscle lysate was cleared by centrifugation and subjected to immunoprecipitation using AMPK α1/α2 antibodies. Immunoprecipitates were maintained on ice either untreated or treated with calf intestine phosphatase (CIP) and then probed by Western blotting using indicated antibodies. Representative Western blots are shown.

Figure 7. AMPKβ2 Thr-148 mutant enhances glycogen content of C2C12 myotubes

C2C12 cells stably overexpressing AMPKβ2-WT or -T148D mutant were differentiated into myotubes for 4-5 days, and subsequently incubated with high (25 mM), low (3 mM) or no (0 mM) glucose for 16 h. **(A)** Myocellular glycogen levels were determined using biochemical glycogen assay, as described in Materials and Methods. * $p<0.01$ vs. WT 25 mM, # $p<0.05$ vs. T148D, $ $p<0.05$, 25 mM,; $n=2$. (**B**) Insulin-stimulated glucose uptake was determined as described in Material and Methods. $ $p<0.01$ vs. WT.

Figure 1.

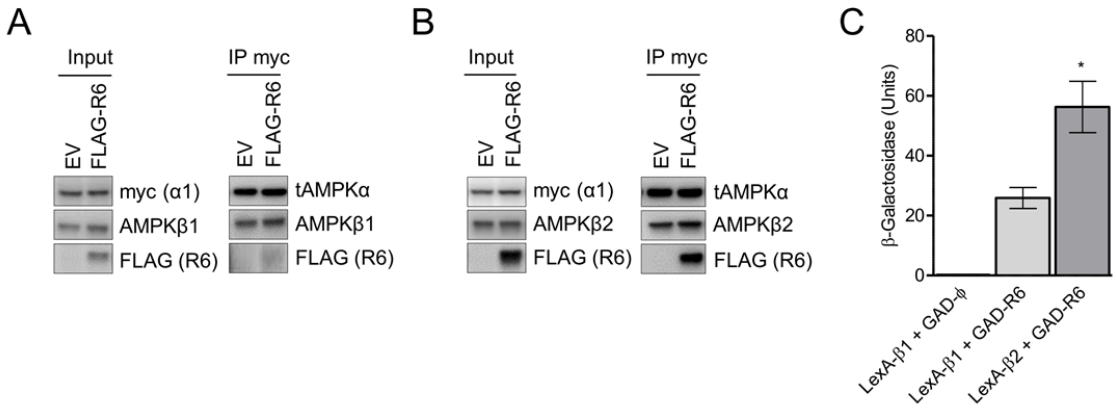
A
Input
IP myc
EV
FLAG-R6
myc (α1)
AMPKβ1
FLAG (R6)
tAMPKα
AMPKβ1
FLAG (R6)
B
Input
IP myc
EV
FLAG-R6
myc (α1)
AMPKβ2
FLAG (R6)
tAMPKα
AMPKβ2
FLAG (R6)
C
β-Galactosidase (Units)
80
60
40
20
0
*
LexA-β1 + GAD-ϕ
LexA-β1 + GAD-R6
LexA-β2 + GAD-R6

Figure 2.

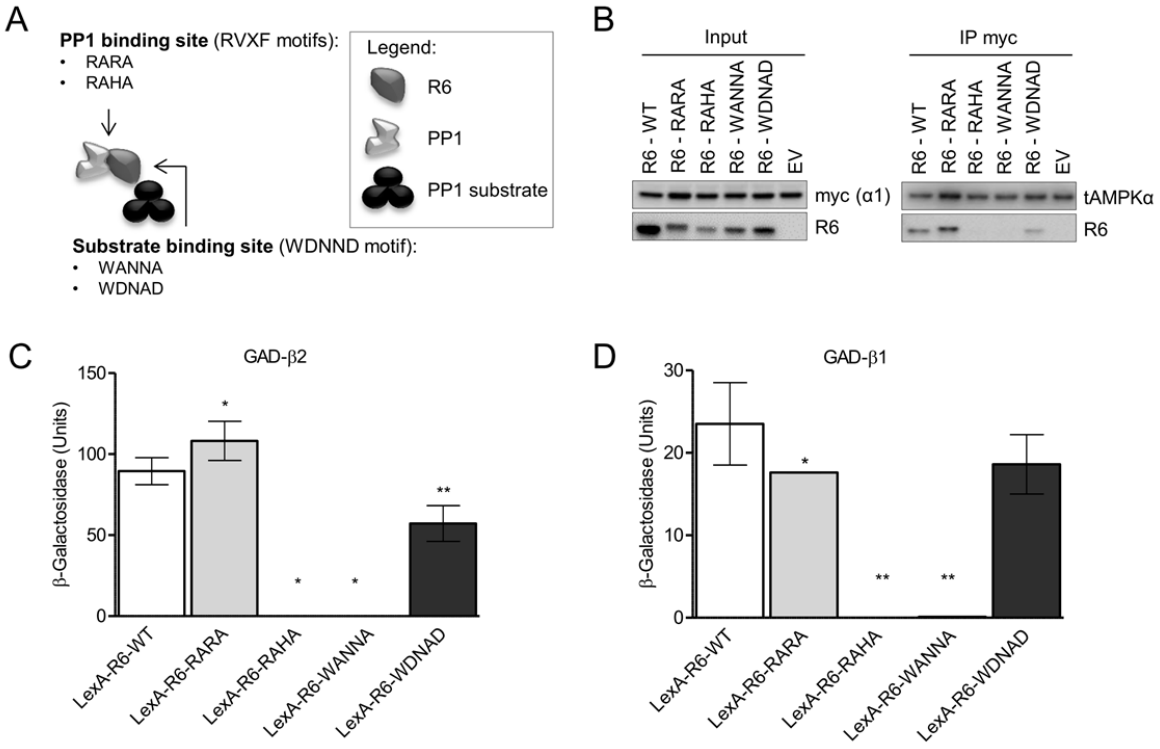
A
PP1 binding site (RVXF motifs):
• RARA
• RAHA
Legend:
R6
PP1
PP1 substrate
Substrate binding site (WDNND motif):
• WANNA
• WDNAD
B
Input
IP myc
R6 - WT
R6 - RARA
R6 - RAHA
R6 - WANNA
R6 - WDNAD
EV
myc (α1)
R6
tAMPKα
R6
C
GAD-β2
β-Galactosidase (Units)
150
100
50
0
LexA-R6-WT
LexA-R6-RARA
LexA-R6-RAHA
LexA-R6-WANNA
LexA-R6-WDNAD
D
GAD-β1
β-Galactosidase (Units)
30
20
10
0
LexA-R6-WT
LexA-R6-RARA
LexA-R6-RAHA
LexA-R6-WANNA
LexA-R6-WDNAD

Figure 3.

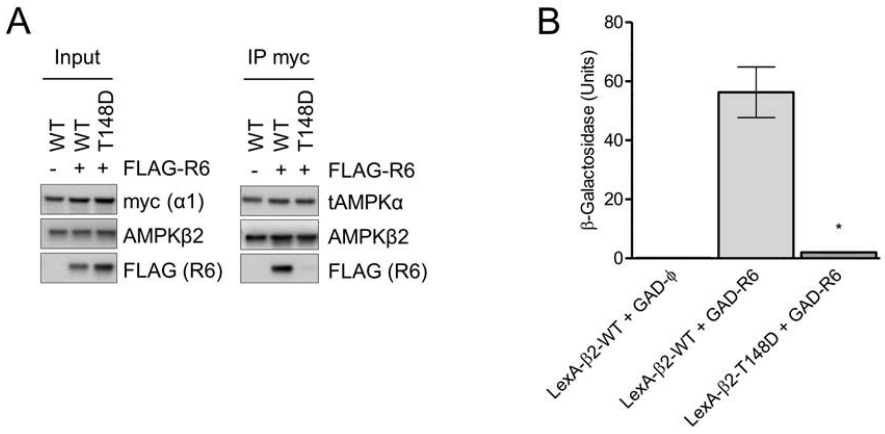
A
Input
IP myc
WT
WT
T148D
- + + FLAG-R6
myc (α1)
AMPKβ2
FLAG (R6)
tAMPKα
B
β-Galactosidase (Units)
80
60
40
20
0
*
LexA-β2-WT + GAD-ϕ
LexA-β2-WT + GAD-R6
LexA-β2-T148D + GAD-R6

Figure 4.

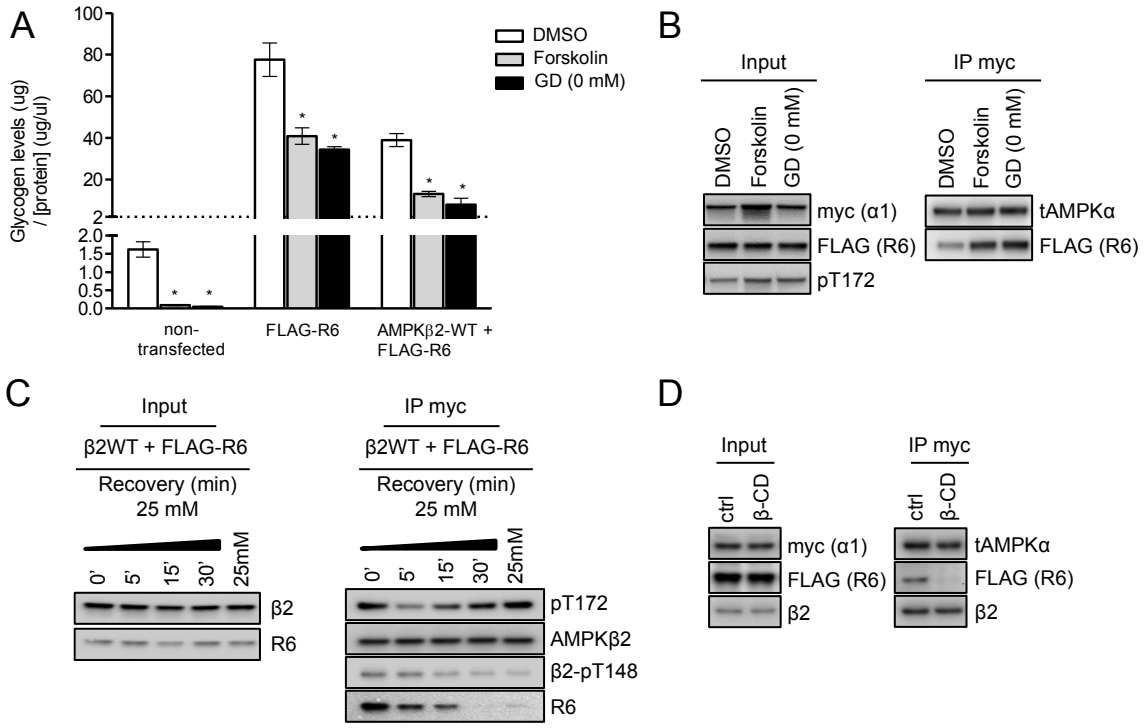
A
Glycogen levels (ug) / [protein] (ug/ul)
DMSO
Forskolin
GD (0 mM)
non-transfected
FLAG-R6
AMPKβ2-WT + FLAG-R6
B
Input
IP myc
DMSO
Forskolin
GD (0 mM)
myc (α1)
FLAG (R6)
pT172
tAMPKα
C
Input
β2WT + FLAG-R6
Recovery (min)
25 mM
0'
5'
15'
30'
25mM
β2
R6
IP myc
pT172
AMPKβ2
β2-pT148
D
ctrl
β-CD
β2

Figure 5.

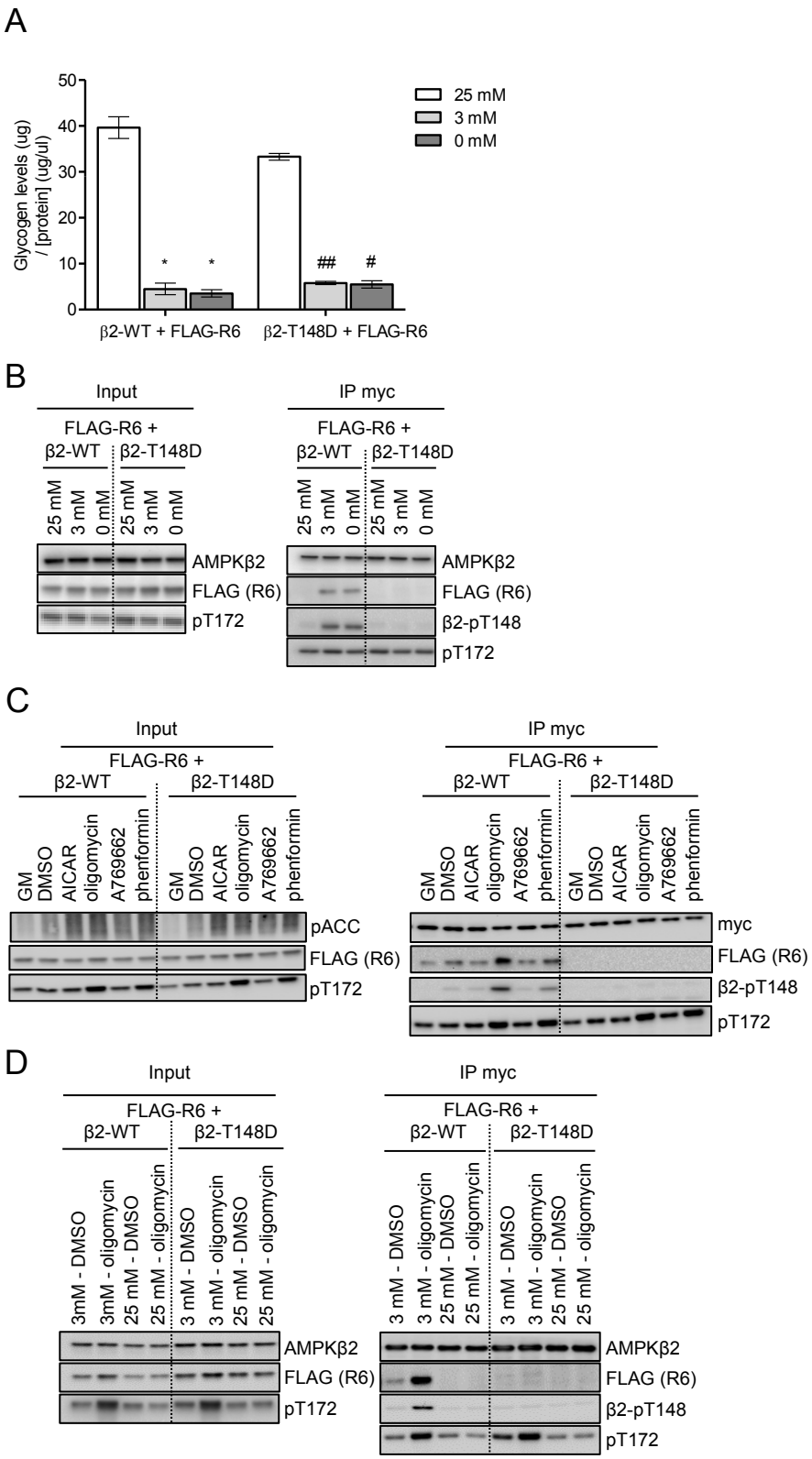
A
Glycogen levels (ug) / [protein] (ug/ul)
25 mM
3 mM
0 mM
β2-WT + FLAG-R6
β2-T148D + FLAG-R6
B
Input
IP myc
FLAG-R6 +
β2-WT
β2-T148D
25 mM
3 mM
0 mM
AMPKβ2
FLAG (R6)
pT172
β2-pT148
C
GM
DMSO
AICAR
oligomycin
A769662
phenformin
pACC
myc
D
3mM - DMSO
3mM - oligomycin
25 mM - DMSO
25 mM - oligomycin
3 mM - DMSO
3 mM - oligomycin

Figure 6.

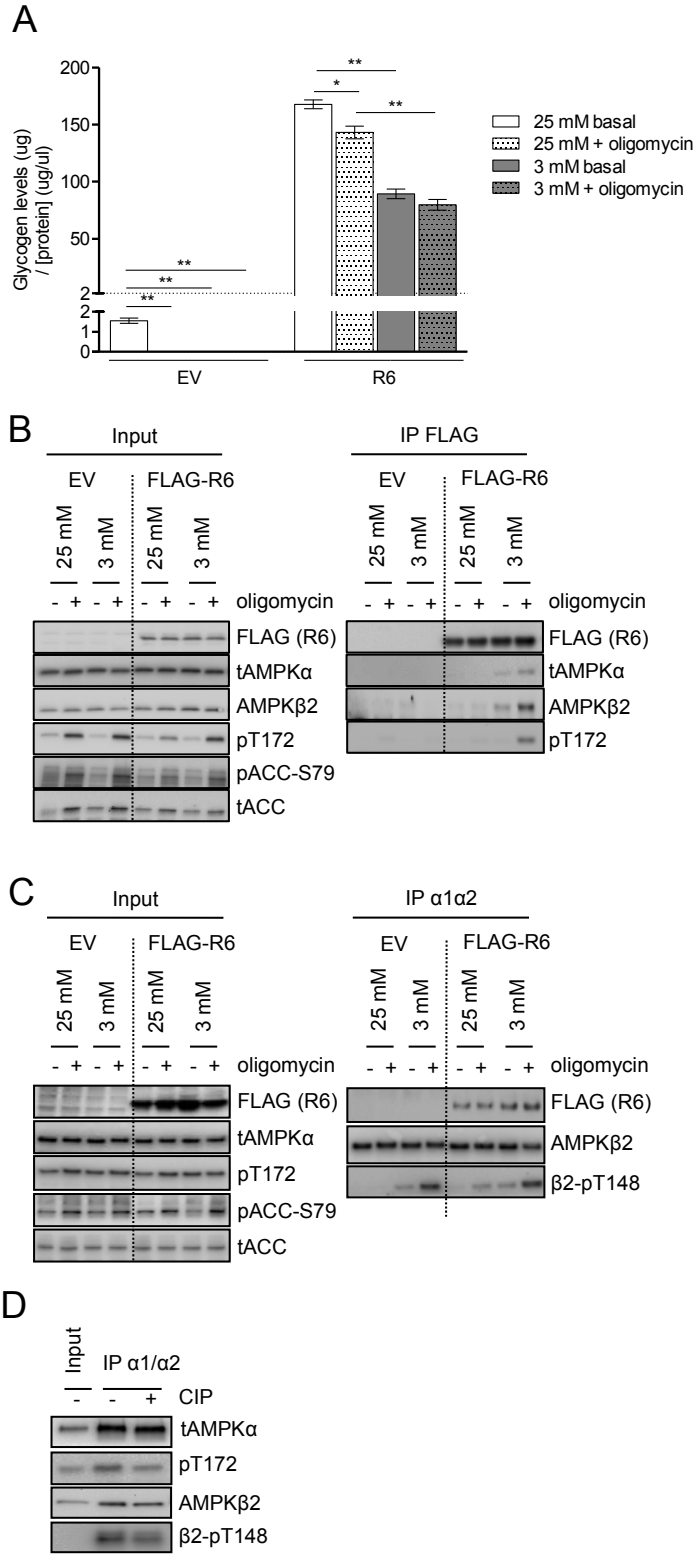
A
Glycogen levels (ug) / [protein] (ug/ul)
25 mM basal
25 mM + oligomycin
3 mM basal
3 mM + oligomycin
EV
R6
B
Input
IP FLAG
EV
FLAG-R6
25 mM
3 mM
oligomycin
FLAG (R6)
tAMPKα
AMPKβ2
pT172
pACC-S79
tACC
C
Input
IP α1α2
β2-pT148
D
Input
IP α1/α2
CIP

Figure 7.

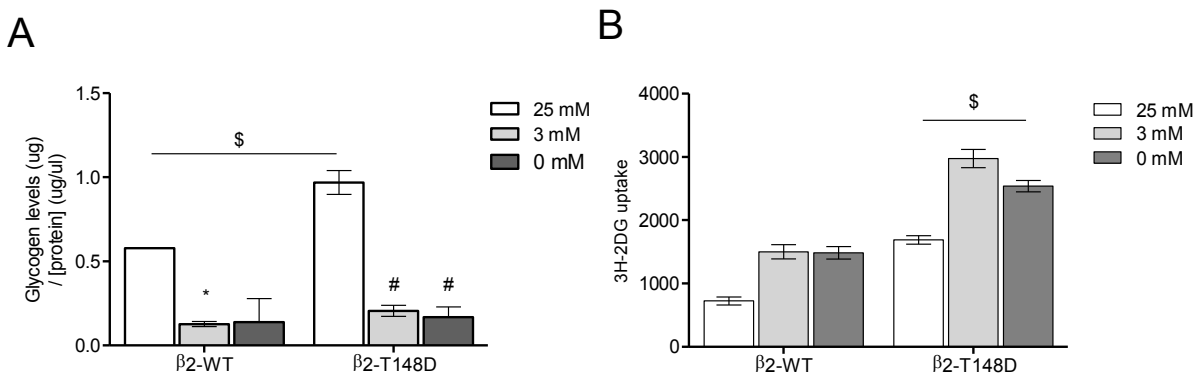
A
B
Glycogen levels (ug) / [protein] (ug/ul)
1.5
1.0
0.5
0.0
$
*
#
#
β2-WT
β2-T148D
25 mM
3 mM
0 mM
3H-2DG uptake
4000
3000
2000
1000
0
$
β2-WT
β2-T148D
25 mM
3 mM
0 mM